Supplementary Information

Table S1: complete list of sample codes, electrospinning parameters and relative properties of the samples

Sample code	Electrospinning parameters				Thickness (µm)	Fiber diameter (µm)	E-modulus (MPa)
	Solution and concentration	Voltage (kV)	Spinning distance (cm)	Spinning time (min)			
PCL7.510152	PCL 7.5% $CHCl_3 + C_2H_6O$ (6:1)	10	15	2	51.25±6.71	2.14±0.63	18.52±4.96
PCL7.510202		10	20	2	N/A	1.97±0.55	N/A
PCL7.510252		10	25	2	N/A	1.91±0.74	N/A
PCL7.515152		15	15	2	66.30±5.26	1.95±0.37	9.00±2.64
PCL7.515202		15	20	2	62.88±6.02	1.95±0.43	N/A
PCL7.515252		15	25	2	N/A	1.87±0.51	N/A
PCL7.520152		20	15	2	37.53±5.30	2.00±0.33	N/A
PCL7.520202		20	20	2	29.94±6.72	1.89±0.30	13.43±3.98
PCL7.520252		20	25	2	N/A	1.81±0.33	N/A
PCL7.525152		25	15	2	83.63±8.53	1.74±0.26	11.49±4.36
PCL7.525202		25	20	2	60.87±6.04	1.82±0.31	7.07±1.16
PCL7.525252		25	25	2	N/A	1.49±0.32	N/A
PCL1010152	PCL 10% $CHCl_3 + C_2H_6O$ (6:1)	10	15	2	166.90±6.79	2.75±0.84	10.70±1.37
PCL1010202		10	20	2	61.04±7.34	2.90±0.25	8.54±1.68
PCL1010252		10	25	2	53.21±8.05	2.96±0.32	N/A
PCL1015152		15	15	2	139.59±12.32	2.87±0.36	19.70±4.81
PCL1015202		15	20	2	43.31±11.18	2.69±0.24	15.84±7.71
PCL1015252		15	25	2	41.60±7.45	2.66±0.24	N/A
PCL1020152		20	15	2	128.05±9.25	2.65±0.32	16.30±3.31
PCL1020202		20	20	2	58.52±8.43	2.52±0.26	16.48±4.64
PCL1020204		20	20	4	92.56±9.53	2.52±0.26	17.75±5.15

PCL1020152		20	15	2	129.05±7.28	2.36±0.27	N/A
PCL1025152		25	15	2	143.42±8.68	2.51±0.25	17.72±7.87
PCL1025202		25	20	2	32.67±12.10	2.50±0.29	52.92±13.29
PCL1025252		25	25	2	18.47±4.85	2.39±0.27	41.39±14.05
PCL12.510152	PCL 12.5% $CHCl_3 + C_2H_6O$ (6:1)	10	15	2	90.38±13.52	3.68±0.90	N/A
PCL12.510202		10	20	2	73.33±11.09	3.92±0.29	N/A
PCL12.510252		10	25	2	81.86±12.30	3.84±0.29	4.72±1.26
PCL12.515152		15	15	2	N/A	3.07±0.42	N/A
PCL12.515202		15	20	2	139.90±18.14	3.45±0.30	11.24±1.44
PCL12.515252		15	25	2	36.18±5.81	3.22±0.28	12.67±2.29
PCL12.520152		20	15	2	119.15±14.80	2.79±0.30	N/A
PCL12.520202		20	20	2	98.70±6.71	3.24±0.31	11.77±4.38
PCL12.520252		20	25	2	43.38±4.87	3.36±0.31	10.14±4.12
PCL12.525152		25	15	2	111.32±7.67	3.59±0.32	N/A
PCL12.525202		25	20	2	79.29±7.60	3.67±0.56	20.53±8.44
PCL12.525252		25	25	2	58.52±6.20	3.39±0.32	9.92±4.62
PCL10+radial	PCL 10% $CHCl_3 + C_2H_6O$ (6:1)	20	20	2	48.60±7.66 + 120 µm filaments	2.52±0.26	N/A
PCL10+filam	PCL 10% $CHCl_3 + C_2H_6O$ (6:1)	20	20	2	48.60±7.66 + 120 µm filaments	2.52±0.26	N/A
SF:PCL_0:1_1020152	PCL 10% HFIP	20	15	2	N/A	1.63±0.35	N/A
SF:PCL_1:1_1010152	SF:PCL=1:1 10%	10	15	2	21.91±0.24	0.88±0.25	38.62±2.62

SF:PCL_1:1_1020102	HFIP	20	10	2	58.54±13.10	0.93±0.22	39.43±15.77
SF:PCL_1:1_1020152		20	15	2	15.93±5.04	0.92±0.18	74.75±11.65
SF:PCL_1:1_4Min		20	15	4	N/A	0.92±0.18	N/A
SF:PCL_1:1_8Min		20	15	8	N/A	0.92±0.18	N/A
SF:PCL_1:1_1030102		30	10	2	50.15±15.39	0.88±0.15	59.07±21.68
SF:PCL_1:1_1030152		30	15	2	18.92±2.99	0.88±0.15	84.88±11.86
SF:PCL_1:2_1015152	SF:PCL=1:2 10% HFIP	15	15	2	15.51±0.52	0.69±0.13	34.84±1.36
SF:PCL_1:2_1020102		20	10	2	39.13±10.28	0.75±0.13	44.93±8.60
SF:PCL_1:2_1020152		20	15	2	14.61±0.45	0.74±0.12	41.65±6.59
SF:PCL_1:2_4Min		20	15	4	N/A	0.74±0.12	N/A
SF:PCL_1:2_8Min		20	15	8	N/A	0.74±0.12	N/A
SF:PCL_1:2_1020202		20	20	2	7.53±0.22	0.71±0.12	28.85±7.02
SF:PCL_2:1_1015152	SF:PCL=2:1 10% HFIP	15	15	2	27.72±1.77	1.02±0.21	74.85±11.98
SF:PCL_2:1_1020102		20	10	2	73.79±31.44	0.94±0.14	44.85±12.88
SF:PCL_2:1_1020152		20	15	2	33.80±5.14	0.98±0.12	62.60±15.64
SF:PCL_2:1_1020202		20	20	2	15.38±1.52	1.03±0.14	35.85±9.78

Self-constructed laser Doppler vibrometer (LDV) test stand for dynamic acoustic vibration

The self-constructed laser Doppler vibrometer (LDV) test stand (**Figure S1**) was used in this work to characterize the dynamic vibration behavior of TM implants. Specimens are fixed with the clamping part assembly and the adjusting wheel, as shown in **Figure S1**. The clamping part assembly consists of a silicone ring and two centrically aligned clamping parts. The applied fixation force are the sum of the weight of the clamping parts and an additional force controlled by an adjusting wheel. The silicone ring has a weight of 4.32 mg that provides a small fixation force of 4.32 mg • 0.001 kg • 9.81 m/s² = 0.4 mN. Together with the two top clamping part, the weight summed up to 0.0432 + 8.3822 = 8.4254 g and results into a fixation force of 8.4254 • 0.001 kg • 9.81 m/s² = 0.0827 N. The total fixation force is defined in terms of radial tension caused by the fixation mechanism at the specimen rim. To determine the radial tension, the strain gauge half-bridges that are attached at the three clamping mechanism beams of a PMMA circle disk, are used to measure the caused strain ξ firstly. Then the total fixation force can be calculated from $F_{total} = 3 \bullet F = 3 \bullet (E \bullet \xi \bullet W / L)$ (E: the E-modulus of PMMA, 3200 MPa; W: the resistance of moment at one of the beam, 0.002 mm³; L: average bending length, 5.5 mm). The magnitude of the strain can be easily tuned by rotating the adjusting wheel. The specimens are excited with a sound signal through a plug-in earphone (ER-2C, Etymotic Research, USA) inserted from the artificial canal. The probe of a measuring microphone (ER-7C, Etymotic Research) is placed about 1 mm in front of the center of the membrane to measure the applied sound pressure. The resulting vibration velocity is measured with a LDV (Polytec, Germany) and then mathematically integrated to obtain the displacement. The transfer function to characterize the vibration behavior is thus obtained as the deflection of the sample center point related to the excitation sound pressure.

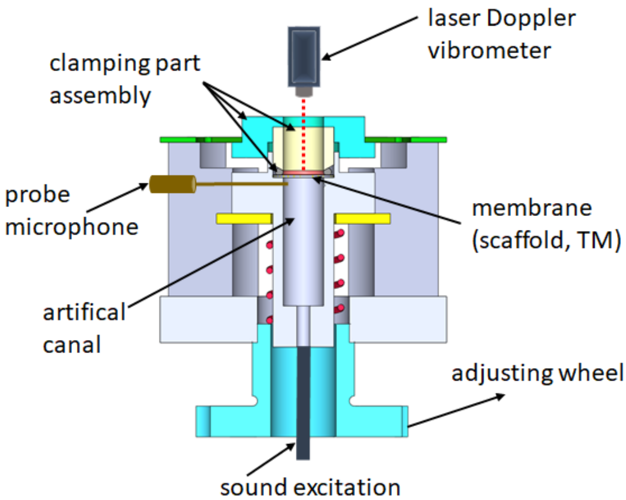

Figure S1: Schematic of self-constructed LDV test stand

Determination of Flow Rate

To determine the flow rate used in this work for PCL and SF:PCL-electrospinning solutions preliminary experiments were performed. There, flowrates between 0.5 ml/h and 2.5 ml/h were analyzed regarding constant solution flow, dripping and multiple electrospinning jets. For PCL and SF:PCL solutions 1.95 ml/h and 0.8 ml/h were selected as flow rates due to consistent spinning properties, respectively. These rates were set constant for all PCL and SF:PCL case groups.

Conductivity measurements

To better understand the origination of the bimodal fiber diameter distribution of SF-PCL-blends, conductivity measurements were performed to validate the existence of left over salts after dialysis. Therefore, the HI98129 Combo Tester (Hanna Instruments Deutschland GmbH, Germany) was placed inside the dialysate after performing the described dialysis protocol. 400 µS could be measured, showing that left over salts were still present.

The conductivity of actual spinning solutions could not be determined due to the lack of a solvent resistant measurement device. While in dialysis, the SF is dissolved in water. After freeze-drying of the dialysate, SF is dissolved in HFIP and blended with PCL to prepare the spinning solution.

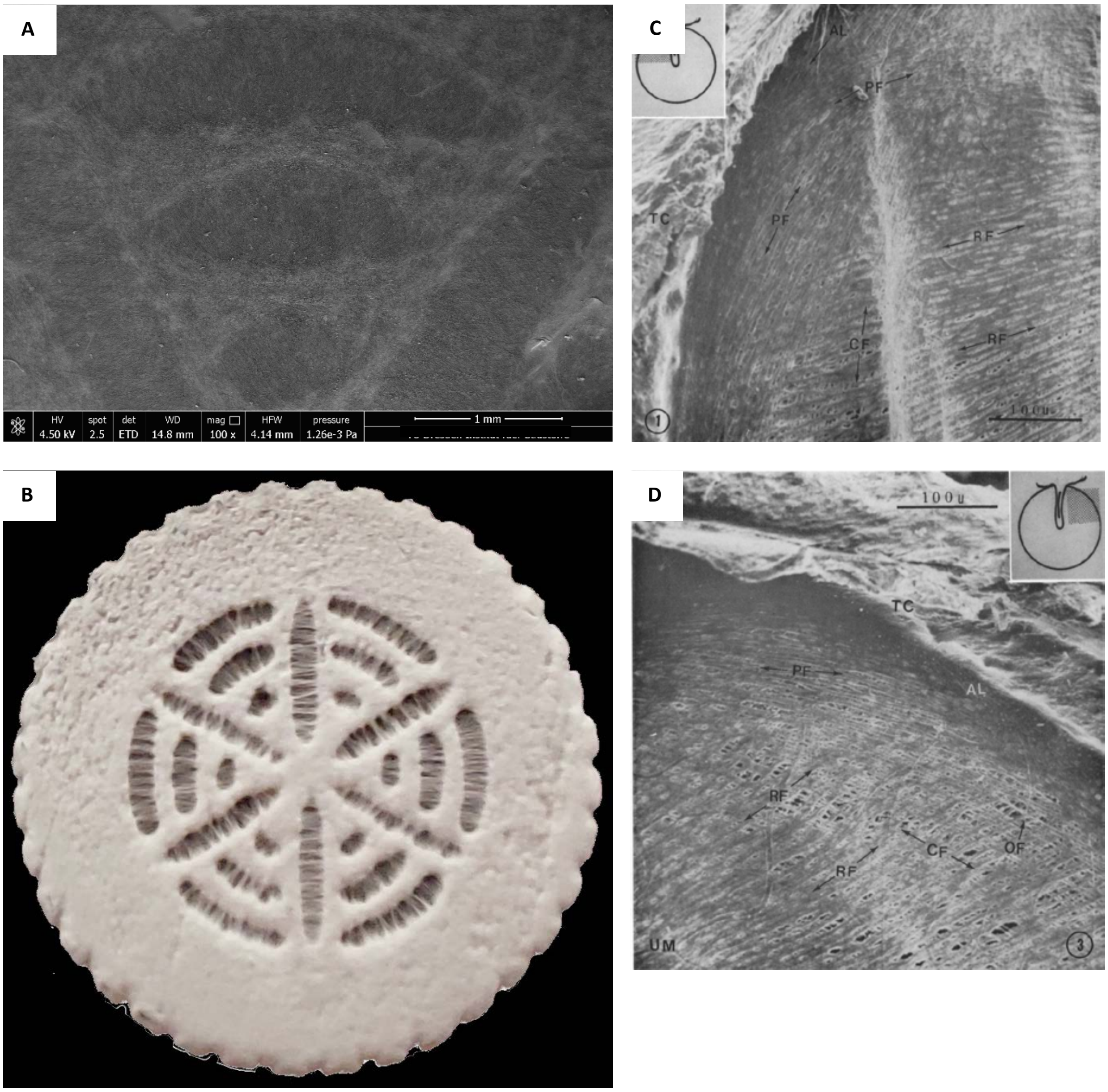

Figure S2: A) SEM-image of radially and circumferentially oriented fibers in TM-sized membrane, see **Figure 5** for corresponding collector design and light microscopy image; **B)** image of full eardrum sized graded membrane structure; **C)** and **D)** SEM images of anterior/ posterior superior quadrant of human TM, clearly showing circumferential and radial fiber alignment (I. Kawabata & H. Ishii (1971) Fiber Arrangement in the Tympanic Membrane: Scanning Electron Microscope Observations, Acta Oto-Laryngologica, 72:1-6,243-254, DOI: 10.3109/00016487109122479)

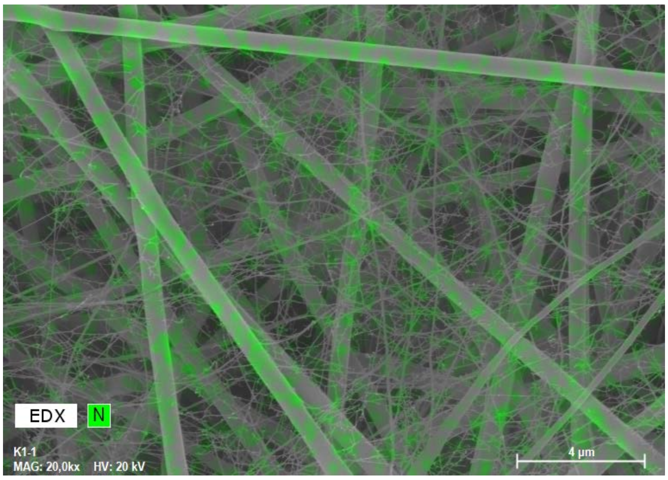

Figure S3: EDX-analysis of SF-PCL-blend membrane including nitrogen mapping (green spots), nitrogen occurs in micro- as well as nano-sized filaments

Tensile tests of specimen with oriented fiber areas

To generate specimen with oriented fiber areas, custom collectors with varying number (1-3) and width (0.5/1.0/1.5 mm) of gaps were designed and used for electrospinning. The collector design is shown in **Figure S4** for 1 mm gap size. The collectors were 8 mm in length and 5 mm in width to match the specimen geometry of randomized electrospun tensile test specimen. The area in between gaps was held constant at 1 mm length, independent of gap number and width.

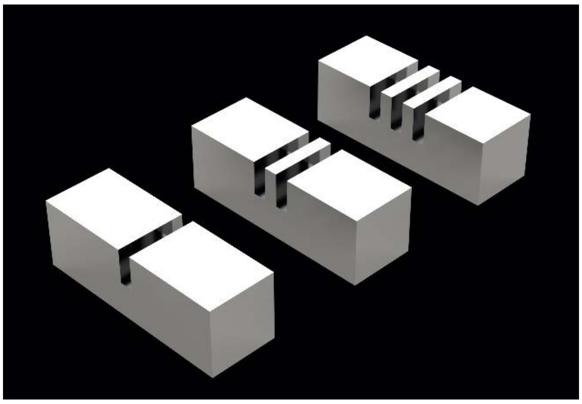

Figure S4: 3D-printed collectors for electrospinning of aligned fiber areas; here exemplary gap width of 1 mm

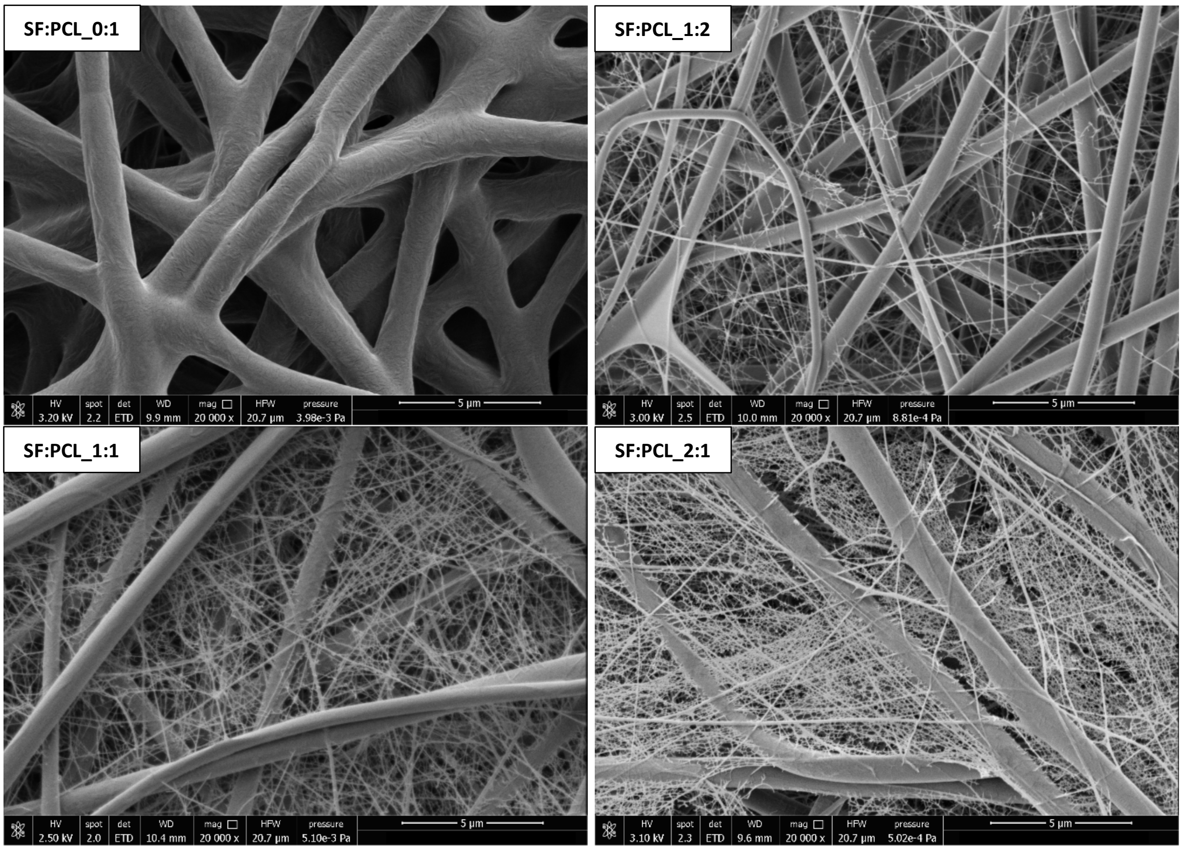

Figure S5: SEM images of membranes with increasing SF-content; nanofiber fraction increases with SF-content

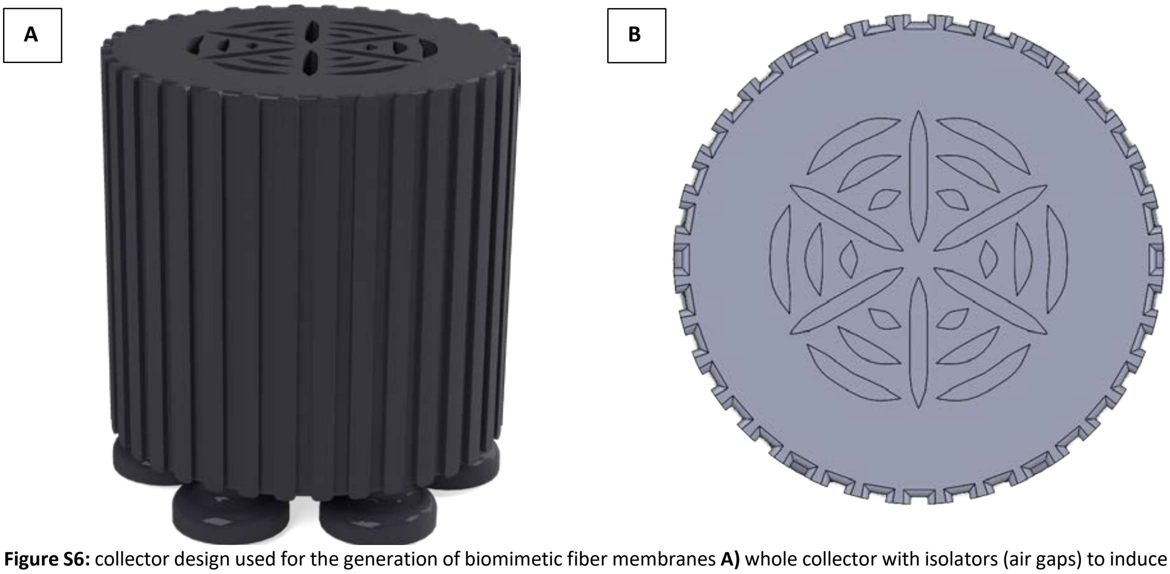

Figure S6: collector design used for the generation of biomimetic fiber membranes **A)** whole collector with isolators (air gaps) to induce fiber orientation and guiding rails for optional integration of precrystallized filaments in linear patterns; **B)** top view to emphasize gap orientation